https://doi.org/10.37434/tpwj2020.12.06

CORROSION AND MECHANICAL RESISTANCE OF WELDED JOINTS OF ALUMINIUM B1341T ALLOY, PRODUCED BY ARGON ARC WELDING USING FREE AND CONSTRICTED ARC

L.I. Nyrkova, T.M. Labur, S.O. Osadchuk and **M.R. Yavorska**
E.O. Paton Electric Welding Institute of the NAS of Ukraine
11 Kazymyr Malevych Str., 03150, Kyiv, Ukraine. E-mail: office@paton.kiev.ua

In the work the results of studies of corrosion and mechanical resistance of welded joints of B1341T alloy with a thickness of 1.2 mm, depending on the technology of manual argon arc welding using free and constricted arc are presented. The strength coefficient of welded joints is 0.79 and 0.8, respectively. Potentiometric measurements established an electrochemical heterogeneity between the base metal and the welded joints produced using free and constricted arc, which is equal to 100 mV and 86 mV, respectively. More positive potential is inherent to the region of a weld with a smaller area, which is safe to operation. Accelerated corrosion tests determined that the shape of the arc column during manual welding does not affect the resistance of welded joints to exfoliating corrosion and a corrosion-mechanical resistance under the conditions of a constant deformation. The level of resistance of the metal to exfoliating corrosion of the joints produced by both types of arc welding technology, was estimated by the point 2–3. The fracture time of the specimens welded by free arc welding, decreased on average to 20 days as compared to the base metal (73 days). The similar results were obtained for the joints welded by a constricted arc. At the same time, it was revealed that the use of constricted arc for welding, causes a decrease in the resistance of the joints to intercrystalline corrosion. The maximum fracture depth of the boundaries' grains is 0.350 mm for the joints produced by a free arc and 0.460 mm for the joints made by a constricted arc. 15 Ref., 3 Tables, 11 Figures.

Keywords: aluminium alloy, free and constricted arc welding, welded joint, mechanical properties, structure, intercrystalline corrosion, exfoliating corrosion, corrosion under constant deformation, potentiometry, accelerated corrosion tests

Aluminium alloys of the Al–Mg–Si–Cu alloying system used in aircraft engineering are characterized by a high manufacturability in combination with the characteristics of strength, weldability and corrosion resistance [1–8]. Such group of alloys includes the alloy of grade B1341T, which is used for the manufacture of structures of cylinders, tanks, where liquid substances are stored [3]. Namely due to this fact it is necessary to provide that the products have the optimal level of both mechanical and corrosion properties. Under the production conditions, individual structural elements of hydraulic tanks after stamping are often joined by manual argon arc welding using a nonconsumable electrode with free or constricted arc [1, 4, 7]. A free arc is characterized by a relatively low penetrating ability. The use of pulsed arc modes improves the shape and size of the welds, the conditions of their solidification, and also helps to reduce the loss of strength of the base metal during welding. Due to a cylindrical shape of the arc column, which is formed as a result of its constriction by a layer of inert gas, during welding with a constricted arc, an increase in heat concentration occurs. In addition, it is known [2–4] that the stability of the weld metal usually does not coincide with the stability of the base metal as a result of the formation of a heterogeneous joint structure during welding. Therefore, the aim of this work is to study the influence of manual welding technology using free and constricted arc on the complex of corrosion and corrosion-mechanical properties of welded joints (WJ) of B1341T alloy to determine the efficiency of these processes.

Procedure of experiments. In the work, aluminium B1341T alloy is used, the chemical composition of which according to spectral analysis performed in the DFS-36 spectrometer, is the following, wt.%: (0.45–0.9) Mg, (0.5–1.2) Si, (0.15–0.35) Mn, (0.1–0.5) Cu, (0.05–0.1) Ca, 0.25 Cr, 0.2 Zn, 0.15 Ti, 0.5 Fe, the content of other elements is not more than 0.1, Al is the base.

The sheet billets of B1341T alloy with a thickness of 1.2 mm before welding were etched in a 10% solution of NaOH and clarified in a 25 % solution of HNO_3, thoroughly washed in running hot and cold water and dried in air. The ends of the workpieces

L.I. Nyrkova — https://orcid.org/0000-0003-3917-9063, T.M. Labur — https://orcid.org/0000-0002-4064-2644,
S.O. Osadchuk — https://orcid.org/0000-0001-9559-0151, M.R. Yavorska — https://orcid.org/0000-0003-2016-6289

were mechanically cleaned with a scraper to a depth of 0.1 mm. Welding of butt joints was carried out along the rolled sheet metal of a semi-finished product. The billets were welded abutt, without a backing, using single-pass manual welding with a filler wire of grade Sv 1217 with a diameter of 1.2 mm in argon (according to GOST 10157 [9]). Figure 1 shows a diagram of the sequence and modes of welding.

Free arc welding was performed at a current of different polarity of a sinusoidal waveform using the MW2000 Fronius inverter, and welding using a constricted arc was performed at an asymmetric current of different polarity of a rectangular waveform and overload of the current duration using the PLASMA POWER SUPPLY, which was designed at the PWI for manual and automatic welding of thin-sheet ferrous and nonferrous metals of 0.3–1.5 mm at direct and alternating current. Welding modes and welding materials are presented in Table 1.

The appearance of the welded joints produced during free and constricted arc welding is shown in Figure 2.

Determination and evaluation of mechanical properties were performed on flat specimens with a technological reinforcement on the facial and back surfaces of the weld. The tests were performed according to [11, 12] in the machine MTS 318-25. The load was applied at a traverse speed movement of 2 mm/min before a fracture. During the tests, the load and deformation indices were continuously recorded, according to which results the values of the corresponding indices were calculated: yield strength, ultimate strength (tensile strength) and elongation. The level of deformation ability of the base metal and welded joints was established by the index of bending angle (α) under the conditions of three-point bending with the application of a load from the root side of the weld in accordance with GOST 6996 [12].

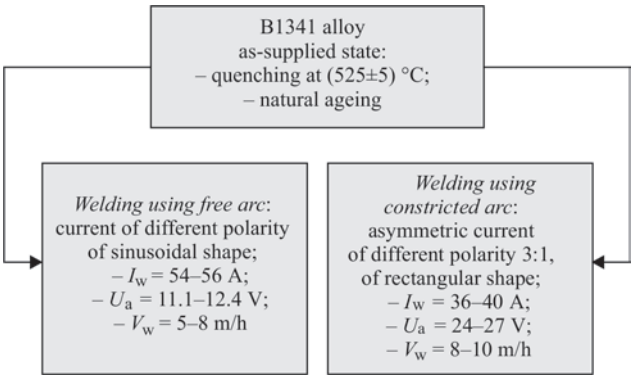

Figure 1. Scheme of sequence of performing operations of producing specimens for investigations and their modes

The microstructure of welded joints was studied on metallographic sections, which were cut out perpendicular to the axis of the welds and prepared according to a standard procedure. To detect the microstructure, electrolytic etching in a solution of the composition: 930 ml of CH_3COOH + 70 ml of $HClO_4$ was used.

Electrochemical investigations were performed by the methods of potentiometry and polarization curves using the potentiostat PI-50-1.1 and the programmer Pr-8. The distribution of potential on the surface of the welded joint was investigated by measuring the potential under the drop in the solution of 3 % NaCl

Table 1. Modes of manual one-sided argon arc welding of B1341T alloy of 1.2 mm thickness using nonconsumable electrode with free and constricted arc

Welding method	Diameter of tungsten electrode, mm	Diameter of filler wire, mm	Argon consumption, l/min	Consumption of shielding gas, l/min	Consumption of plasma-forming gas, l/min	Ratio of direct and reverse polarity
Free arc [10]	1.6	2.0–2.5	7–8.0	–	–	–
Constricted arc	1.6	2.0	4.0–8.0	3.0–6.0	0.8–1.5	3/1

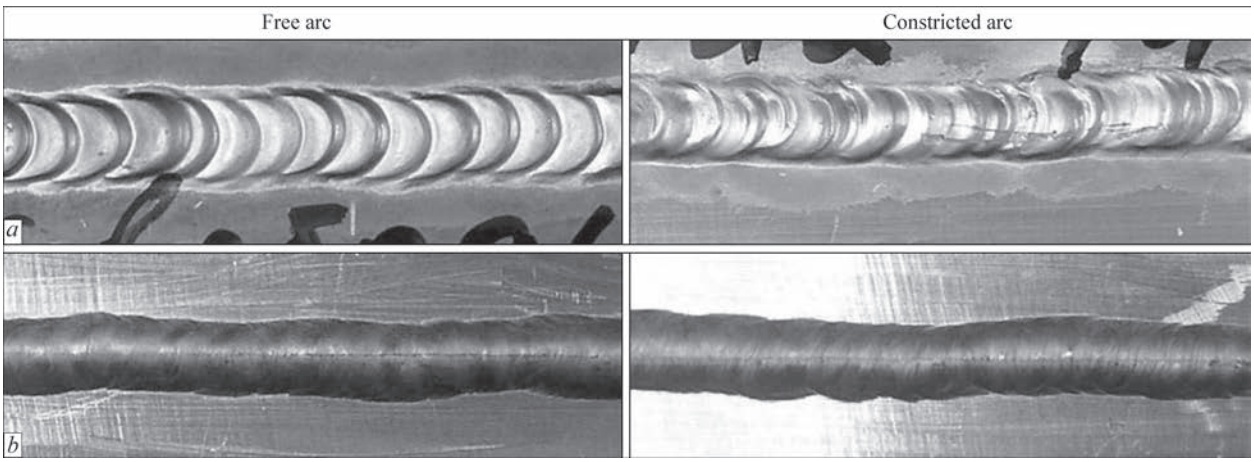

Figure 2. Appearance of as-welded joints: *a* — facial weld surface; *b* — weld root

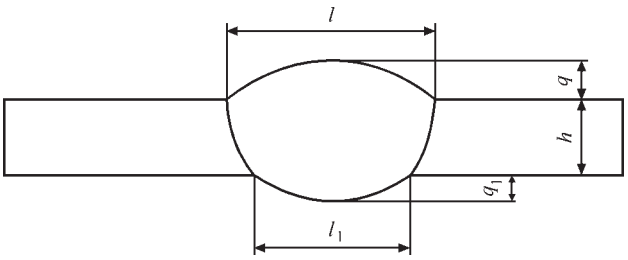

Figure 3. Scheme of measuring geometric dimensions of welds to calculate its form factor

according to the procedure developed at the PWI. To analyze the polarization curves, a clamping electrochemical cell was used. The working electrode was different zones of the welded joint, the reference electrode was a saturated silver chloride electrode EVL-1M1 and the auxiliary electrode was platinum. Polarization curves were recorded in a potentiodynamic mode at a potential scanning rate of 0.5 mV/s in the solution of 3 % NaCl. Before measurements, the surface of specimens was treated with a sandpaper and degreased with ethyl alcohol.

The resistance to intercrystalline (ICC) and exfoliating corrosion was evaluated according by the standard procedures in accordance with GOST 9.021 [13] and GOST 9.904 [14].

The corrosion cracking resistance was investigated in accordance with GOST 9.019 [15]. The tests were performed under the presence of a constant axial tensile stress at the level of 160 MPA at a complete immersion of the specimens of welded joints in the solution of 3 % NaCl in the installation Signal. The test specimens were perpendicularly arranged relatively to the direction of the loading vector action. The duration of the tests was at least 45 days.

Results and their discussion. *Geometric parameters of welds and form factor.* After producing dissimilar joints with the use of different technological methods of manual welding with free and constricted arc, the geometric dimensions of the welds were determined. The explanation of their determination is

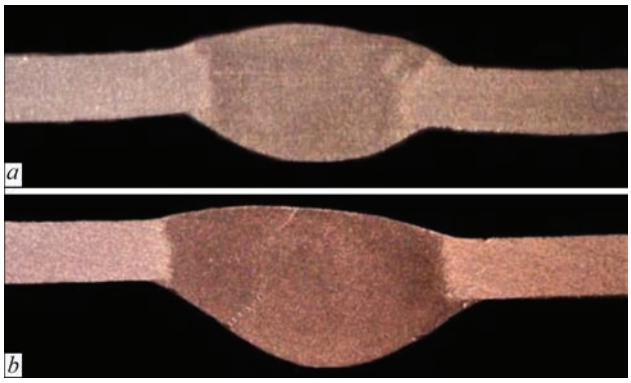

Figure 4. Macrosections of welded joints of B1341 alloy produced by manual argon arc welding at different technological methods of welding using nonconsumable electrode: *a* — free arc; *b* — constricted arc

given in Figure 3, and the obtained results are shown in Table 2. The form factor of the weld was calculated by the formula: $K = l/t$, where $t = h + q$, t is the thickness of the weld; l is the width of the weld; q is the height of reinforcement; h is the greatest depth of the molten base metal.

Analysis of the calculation results showed that weld form factor of the welded joint produced by a constricted arc is approximately 4 % higher as compared to the welded joint produced by a free arc, i.e. it has a little effect on the plane of welds intersection.

Macro- and microstructure of welded joints. Below the results of the study of the macro- and microstructure of the base metal and welded joints of B1341T alloy, produced by free and constricted arc are presented (Figures 4 and 5).

Metallographic examinations established that the microstructure of the base metal of B1341T alloy consists of a saturated solid solution, precipitations of the Mg_2Si phase and coarse inclusions of insoluble intermetallics, which enter the metal at the metallurgical stage of semi-finished product manufacturing (Figure 5, *a*). During arc welding of B1341T alloy, structural transformations take place in the metal, as a result of which three structural zones are formed: weld (Figure 5, *a*),

Table 2. Geometric parameters and form factor of welds produced by free and constricted arc during manual welding of B1341 alloy with a thickness of 1.2 mm

Welding method	Designation of parameters	Geometrical parameters of welds, mm				Weld form factor
		Minimum	Average	Maximum	Average	
Manual welding using free arc	l	3.53–4.86	4.68	4.92–5.60	5.2	2.43
	l_1	3.15–4.15	3.84	4.2–5.1	4.55	
	q	0.23–0.70	0.47	0.8–1.3	0.94	
	q_1	0.17–0.68	0.5	0.85–1.15	0.91	
Manual welding using constricted arc	l	3.99–4.80	4.42	4.9–5.5	5.17	2.52
	l_1	3.52–4.50	4.04	4.65–5.35	4.89	
	q	0.15–0.56	0.38	0.6–1.3	0.85	
	q_1	0.35–0.58	0.48	0.75–15	0.97	

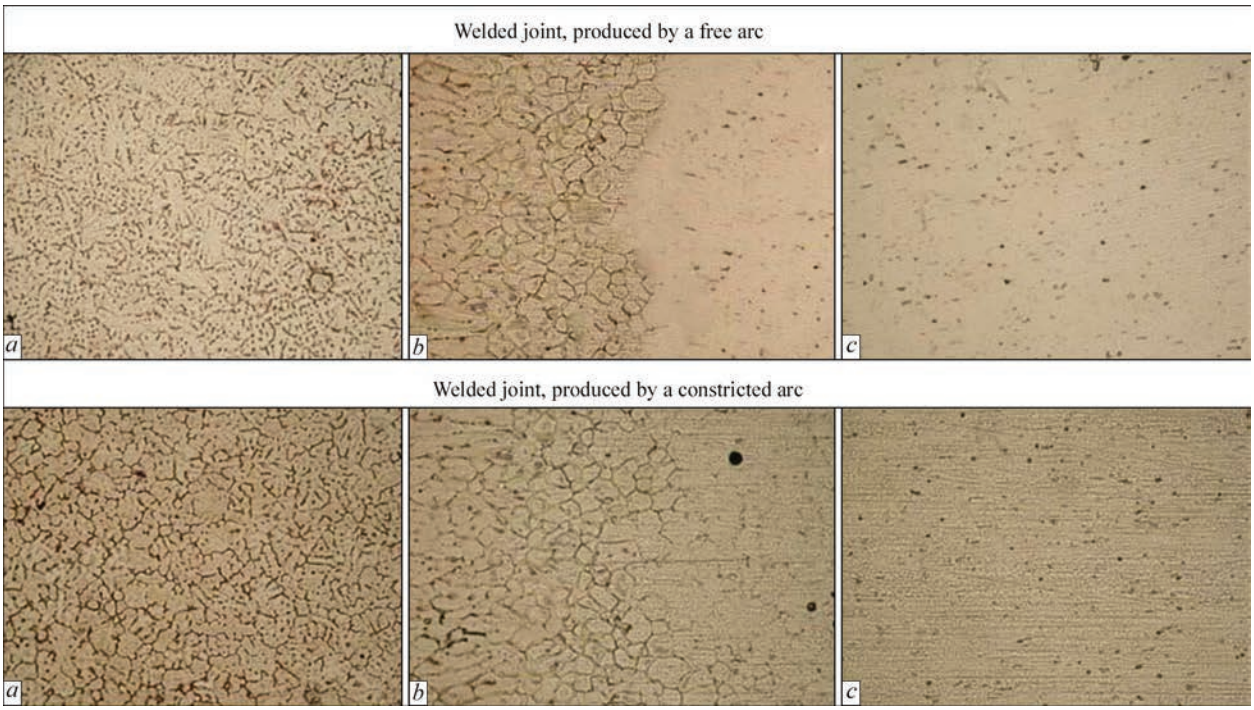

Figure 5. Microstructure (×320) of different zones of welded joints of B1341T alloy, produced by constricted and free arc: *a* — weld; *b* — fusion zone; *c* — base metal

fusion zone and heat-affected-zone (HAZ) (Figure 5, *b*). The structure of the welds of the specimens after welding is homogeneous with the characteristic arrangement of phases and consists of small dendrites (Figure 5, *a*). In the volume of the welds, coarse defects and discontinuities are not observed.

Metallographic analysis of the macrostructure of B1341T alloy joints showed that its welds are characterized by a sufficiently high quality, as there are no coarse defects. In contrast to the base metal (Figure 5), in the welded joint three characteristic parts of the structure are observed, which reflects the degree of influence of the thermal welding cycle on the metal.

The welds have a homogeneous fine-dendritic structure regardless of the arc shape. The size of the dendrites varies in the range of 0.25–0.38 μm. In the process of solidification, the presence of a significant amount of alloying elements and impurities in the composition of the base material and filler wire causes the formation of a significant amount of phases that are uniformly arranged across the joints, but differ in size and shape. According to the state diagram of the system Al–Mg–Si–CuFe in an equilibrium with a solid solution (matrix), such metastable phases can be located as Mg_2Si, $SiCuAl_2$, $FeAl_3$, Mg_5Al_8, and: $CuFeA1_5$, $CuMgAl_2$, $FeSiAl_5$, $FeMg_3Si_6$. The intercrystalline layers are mostly dense and have more distinct contours.

The microstructure of the fusion zone of the weld with the base metal is characterized by the presence of the flashed grain boundaries formed under the conditions of welding heating. This is accompanied by thickening of the boundaries as a result of contact melting of grains with each other and under the conditions of a high-temperature welding heating the formation of the eutectic Mg_2Si phase, located along the grain boundaries (Figures 4, 5). Dissolution of some strengthening phases is also noted. In the structure of HAZ under the action of the thermal cycle of welding, separate fragments of grain boundary flashing and a partial precipitation of secondary phases and eutectics are observed. In addition, coarsening (coagulation) of inclusions of insoluble harmful phases takes place, which reduces the strength of the metal in HAZ.

It should be noted that during welding by a free arc, the width of the HAZ decreases. It can be assumed that such a joint will have a higher corrosion resistance under operating conditions due to a lower heterogeneity of the product.

Mechanical investigations. The mechanical properties of the specimens produced using different technological methods are presented in Figure 6. The analysis of the obtained results shows that the specimens of the base metal are fractured in the working area, and the fracture of specimens of both types of welded joints occurs in the HAZ at a distance of 3–5 mm from the fusion boundary. As compared to the strength of the base metal, the level of these characteristics for welded joints is lower by 22 and 20 %, the yield strength is by 30 and 23 %. The coefficient of strength of welded joints is 0.79 and 0.8. The difference in the shape of the arc has a stronger effect on the characteristics of ductility. Thus, the bending

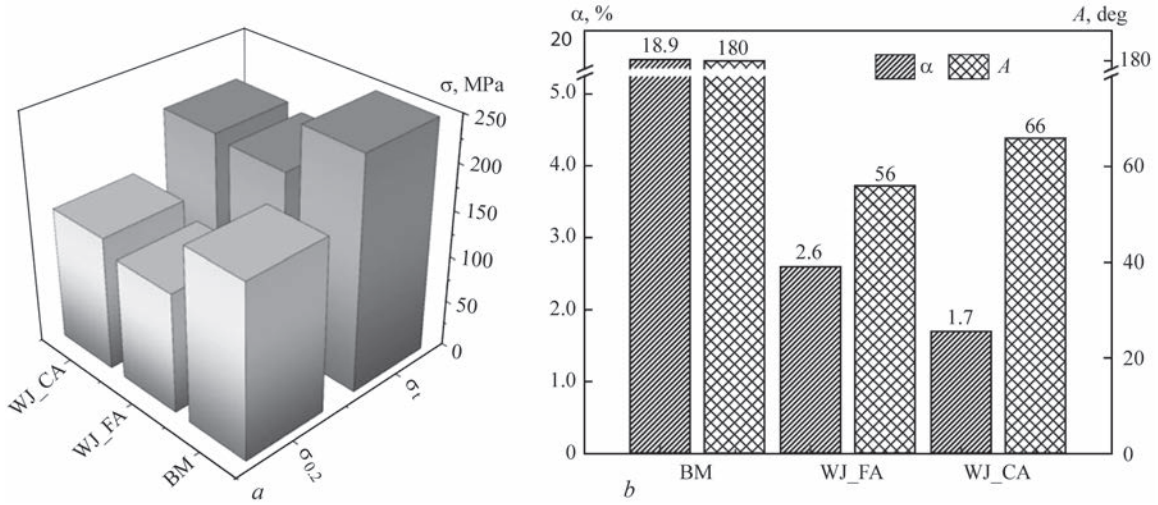

Figure 6. Mechanical properties of welded joints and base metal: *a* — tensile and yield strength; *b* — elongation and bending angle (WJ_CA — welded joint produced by a constricted arc; WJ_FA — welded joint produced by a free arc; BM — base metal)

angle is reduced by 70 and 63 %, and the elongation is by 86 and 91 %. Thus, the joint produced by a constricted arc has a higher tensile strength, ductility and bending angle as compared to the joint produced by a free arc, but the value of the elongation is less than in Figure 6. Probably, this is connected with coarsening (coagulation) of inclusions of insoluble harmful phases as a result of the action of the thermal cycle of a constricted arc welding. Thus, a constricted arc welding contributes to some extent to the strength of welded joints, but at the same time a decrease in the level of ductility is noted.

Electrochemical investigations. The corrosion potential of the base metal is almost –0.729 V. The potential difference between the base metal and the weld is 0.100 V and 0.08 V for the joints produced by free and constricted arc, respectively (Figure 7). Therefore, the potential difference is quite high, but a corrosion potential of the weld is more positive than that of the base metal. The potential difference between the base metal and HAZ is within the values of 0.100 V for the joint produced by a free arc and 0.086 V for that produced by a constricted one, which are admissible by GOST 9.005 (Figure 7, curves *1* and *2*).

From the analysis of experimental results it follows that both types of welded joints have an electrochemical heterogeneity. However, the more positive potential is inherent to the zone with a smaller area and does not represent a danger during operation. Electrochemical heterogeneity between the base metal and the HAZ occurs also in the joints produced by both technologies, which should be taken into account during operation of a welded structure.

Polarization curves measured on the base metal and the weld are presented in Figure 8. It is seen from Figure that the anode and cathode curves, obtained on the welds of both joints, coincide, which is quite natural. The current of anode dissolution on the weld of the specimens of both welded joints (Figure 8, curves *2*, *3*) is much higher than that on the base metal. The cathode curves of the welds are shifted to a region of lower currents as compared to the base metal. In

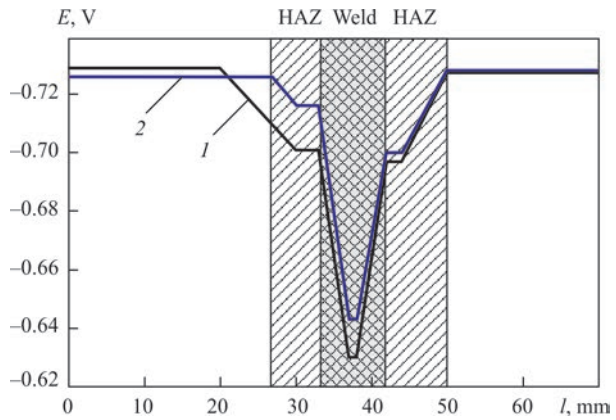

Figure 7. Nature of distribution of potentials under the drop at different zones of welded joint of B1341T alloy, produced by different technological methods: *1* — free arc; *2* — constricted arc

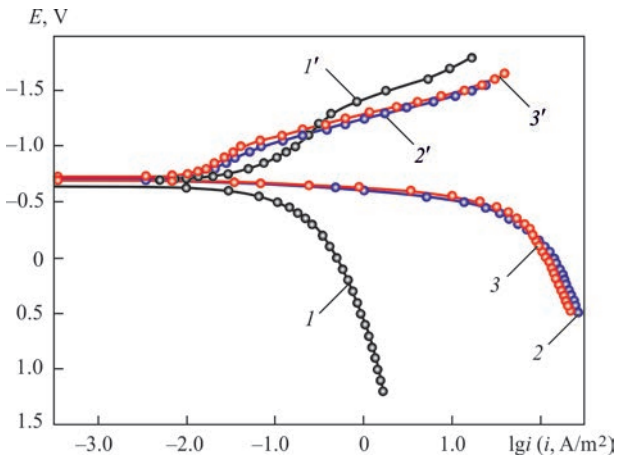

Figure 8. Anode (*1*, *2*, *3*) and cathode (*1′*, *2′*, *3′*) polarisation curves of base metal and weld on welded joint of B1341T alloy: *1* — base metal; *2* — weld of the joint produced by a free arc; *3* — weld of the joint produced by a constricted arc

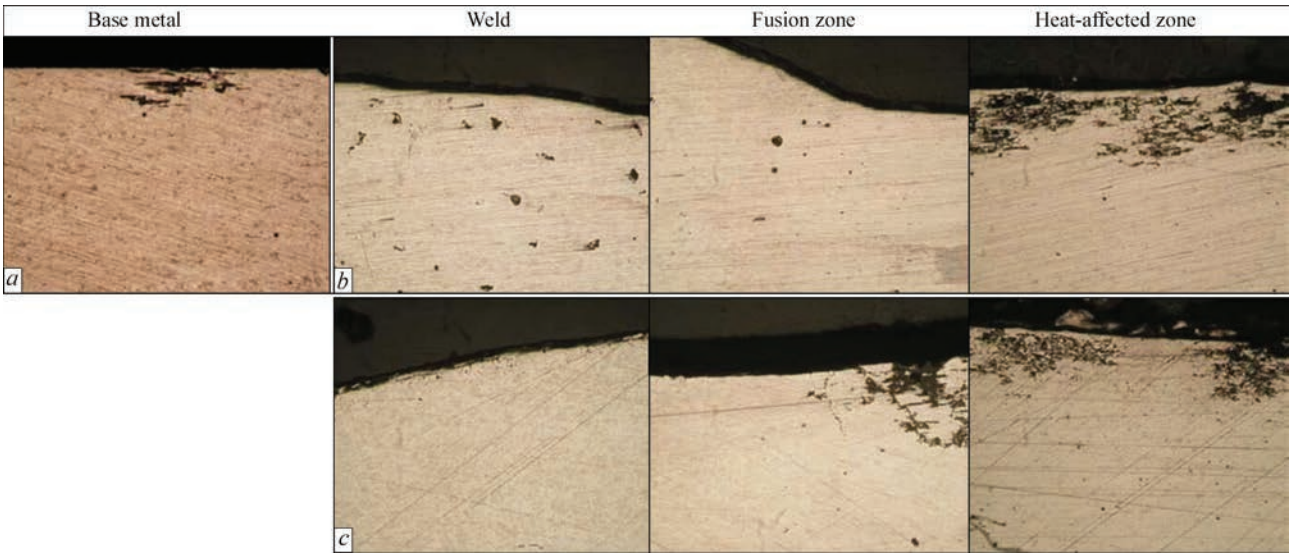

Figure 9. Microstructure (×320) of zones of welded joints of B1341 alloy after the tests on resistance to intercrystalline corrosion: *a* — base metal; *b* — welded joint produced by a free arc: *c* — welded joint produced by a constricted arc

aqueous media at a free access of oxygen, the corrosion process occurs with an oxygen depolarization (Figure 8, curves *1′–3′*). The decrease in the values of the limiting diffusion current on the welds as compared to the base metal indicates a local inhibition of the corrosion process in this area of the welded joint.

Thus, it was revealed that the influence of the applied technological methods of welding almost does not affect electrochemical characteristics of the welded joint.

Resistance to intercrystalline corrosion. The study of resistance to intercrystalline corrosion (ICC) of the base metal showed that the depth of damage to the grain boundaries varies from 0.082 to 0.086 mm. Intercrystalline fracture of the welded joint produced by a free arc was not observed in the area of the weld and the fusion zone (Figure 9, *b*, *c*), but was recorded in the HAZ.

The depth of the damage of the grain boundaries varies from 0.245 to 0.350 mm (Table 3).

On the welded joint produced by a constricted arc, intercrystalline corrosion of the weld was not detected (Figure 9, *b*, *c*). The areas of intergranular fracture are observed in the fusion zone and were propagated to a depth of 0.222 to 0.506 mm and in the HAZ to a depth of 0.222–0.416 mm. Thus, structural transformations and coagulation of insoluble inclusions of harmful phases not only cause a decrease in the strength of the HAZ metal, but also lead to an increase in the local stress at the grain boundaries and, as a consequence, the appearance of a center of intergranular fracture. Thus, the use of welding of thin-sheet metal of B1341T alloy by a constricted arc can reduce the resistance of the welded joint metal to intercrystalline corrosion.

Resistance to exfoliating corrosion. The results of the study of exfoliating corrosion resistance (Figure 10) showed that on the surface of the base metal a change in surface color and delamination with a diameter of not more than 1 mm was revealed. Their total area does not exceed 1.5 % (Figure 10). Delamination at the ends was not detected. According to GOST 9.904, resistance of the base metal of B1341T alloy

Table 3. Mechanical, corrosion and corrosion-mechanical properties of base metal and welded joints of B1341T alloy, produced by free and constricted arc

Condition	Properties of base metal and welded joints							
	Mechanical					Corrosion		Corrosion-mechanical
	σ_t, MPa	$\sigma_{0.2}$, MPa	δ, %	α, deg	Coefficient of WJ strength	Depth of intercrystalline corrosion, mm	Resistance to exfoliating corrosion, point	Time of fracture, days
Base metal	250.5	187.6	18.9	180	–	from 0.082 to 0.086	2–3	from 67 to 88
WJ produced by a free arc	195.0	130.1	2.6	56	0.79	from 0.245 to 0.350	2–3	from 10 to more than 45
WJ produced by a constricted arc	200.3	144.3	1.7	66	0.80	from 0.289 to 0.467	2–3	from 9 to more than 45

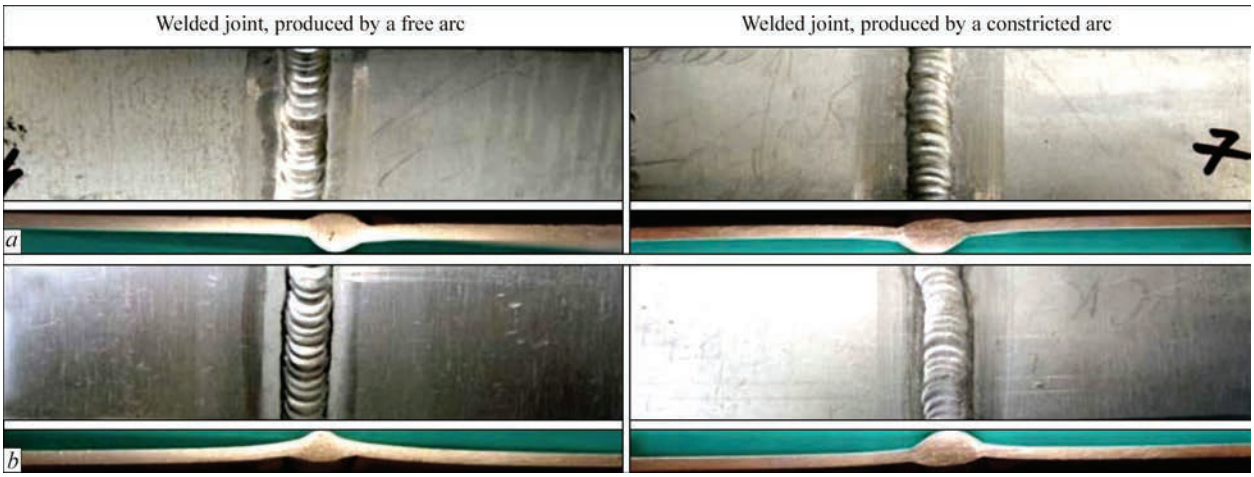

Figure 10. Appearance of working surfaces of specimens of welded joints of B1341T alloy in the state after welding before (*a*) and after (*b*) studies of resistance to exfoliating corrosion (×5)

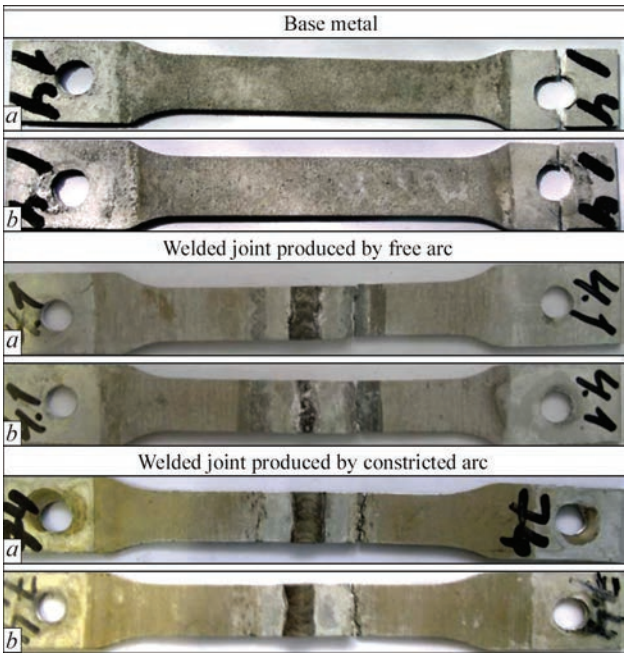

Figure 11. Appearance of specimens of base metal and welded joints of B1341T alloy, produced by free and constricted arc after tests on resistance to corrosion cracking: *a* — facial surface; *b* — back surface

to exfoliating corrosion was evaluated by 2–3 points according to a ten-point scale (Table 3). For welded joints, the condition of the HAZ and weld zone was evaluated. On the surface of the welded joints of both types, delamination in the HAZ and on the weld are also absent. In accordance with the recommendations of GOST 9.904, their resistance to exfoliating corrosion was evaluated by the point I. As far as the resistance of the base metal is slightly lower than that of the area of the weld and HAZ, the resistance of the weld to exfoliating corrosion is generally evaluated by a point 2–3. It was revealed that the peculiarities of the technology of manual argon arc welding using free or constricted arc do not affect the resistance of welded joints to exfoliating corrosion.

Resistance to corrosion cracking. The appearance of the testing specimens after corrosion tests is presented in Figure 11, *a*, *b*. As is seen, on the entire surface of the specimens pittings were formed. In the area of the welded joint, pittings are concentrated mainly in the area of the HAZ, which may indicate the localization of corrosion namely in this part of the welded joints of B1341T alloy. The corrosion-mechanical resistance of the base metal and welded joints in the conditions of joint impact of a constant load at a full immersion in a corrosive environment differs quite significantly (Table 3). A significant scattering of experimental data for both base metal as well as for welded joints is observed. The time before fracture of the base metal specimens ranged from 67 to 88 days (almost 73 days) and for the welded joints produced by a free arc, a decrease in the fracture time to 10–45 days (in average 20 days) was observed. The similar results were obtained for the welded joints produced by a constricted arc. In both cases, the fracture time of the joints made by different welding technologies is almost three times lower than of the base metal. Therefore, the change in technological methods for welding the alloy will not significantly affect the value of a corrosion and mechanical resistance of specimens of welded joints.

Conclusions

According to the results of complex studies of mechanical and corrosion-mechanical properties of welded joints of B1341T alloy with a thickness of 1.2 mm, produced by argon arc welding using free and constricted arc, it was revealed that:

- the strength coefficient of the welded joints produced by free and constricted arc is 0.79 and 0.8, respectively. Thus, the joint produced by a constricted arc has a higher tensile strength and ductility (bending angle) as compared to the joint produced by a free arc, but the values of elongation decrease;
- based on the results of electrochemical investigations, it was determined that after applying both types

of technology, the specimens of welded joints have an electrochemical heterogeneity. At the same time, more positive potential is inherent to the zone of a weld, which has a smaller area, which does not represent a danger during operation;

• it was revealed that the peculiarities of the technology of manual argon arc welding do not affect the resistance of welded joints of B1341T alloy to exfoliating corrosion and corrosion-mechanical strength under the constant deformation. At the same time, the use of a constricted arc welding causes a decrease in the resistance of welded joints to intercrystalline corrosion;

• it was experimentally proved that the corrosion resistance of the welded joint produced by a constricted arc is slightly lower than in the specimens produced by a free arc, but it can be assumed that a well chosen heat treatment of such joints can improve its resistance.

The work was carried out with the support of the National Academy of Sciences of Ukraine within the framework of the program of departmental order of the E.O. Paton Electric Welding Institute in 2017–2021 (state registration number 0117U001188).

1. Feigenbaum, Yu.M., Dubinsky, S.V.(2013) Influence of accidental operational damage on strength and residual life of aircraft structures. *Nauchny Vestnik MGTU GA*, 187, 83–91 [in Russian].
2. Krivov, G.A., Ryabov, V.R., Ishchenko, A.Ya. et al. (1998) *Welding in aircraft construction*. Moscow, MIIVTs [in Russian].
3. Ishchenko, A.Ya., Labur, T.M. (2013) *Welding of modern structures from aluminium alloys*. Kyiv, Naukova Dumka [in Russian].
4. Ovchinnikov, V.V., Grushko, O.E. (2005) High tech welded aluminium alloy V1341 of Al–Mg–Si system. *Mashinostroenie i Inzhenernoe Obrazovanie*, **3**, 2–11 [in Russian].
5. J. Zheng, B., Wang, Q. (1993) lv he jin deng li zi hu li han chuan kong rong chi wen ding jian li tiao jian. *Transact. of the China Welding Inst.*, **3**, 164–171.
6. Martinez, L.F., Marques, R.E, Mcclure, J.C., Nunes, A.C. (1992) Front side keyhole detection in aluminium alloys. *Welding J.*, 71(**5**), 49–52.
7. Norlin, A. (2000) A century of aluminium — a product of the future. *Svetsaren*, 2(**2**), 31–33.
8. Albert, D. (1993) Aluminium alloys in arc welded constructions. *Welding World Magazine*, 32(**3**), 97–114.
9. *GOST 10157–79: Gaseous and liquid argon. Specifications*. Moscow, Izd-vo Standartov [in Russian].
10. Koval, V.A., Labur, T.M., Yavorska, T.R. (2020) Properties of joints of V1341T grade alloy under conditions of TIG welding. *The Paton Welding J.*, **2**, 35–40.
11. *GOST 1497–84: Metals. Test methods on tension.* Moscow, Izd-vo Standartov [in Russian].
12. *GOST 6996–66: Welded joints. Methods of mechanical properties determination*. Ibid. [in Russian].
13. *GOST 9.021–74: Unified system of corrosion and ageing protection. Aluminium and aluminium alloys. Methods of accelerated tests for interctystalline corrosion*. Ibid. [in Russian].
14. *GOST 9.904–83: Unified system of corrosion and ageing protection. Aluminium alloys. Methods of accelerated tests for exfoliating corrosion.* Ibid. [in Russian].
15. *GOST 9.019–74: Unified system of corrosion and ageing protection. Aluminium and magnesium alloys. Methods of accelerated tests for corrosion cracking*. Ibid. [in Russian].

Received 12.11.2020